Structural modulation, hole distribution, and hole-ordered structure of the incommensurate composite crystal $(Sr_2Cu_2O_3)_{0.70}CuO_2$

Y. Gotoh, I. Yamaguchi, Y. Takahashi, J. Akimoto, and M. Goto
National Institute of Advanced Industrial Science and Technology (AIST), Higashi 1-1-1, Tsukuba, Ibaraki 305-8565, Japan

M. Onoda
National Institute for Material Science (NIMS), Namiki 1-1, Tsukuba, Ibaraki 305-0044, Japan

H. Fujino, T. Nagata, and J. Akimitsu
Department of Physics, Aoyama-Gakuin University, Fuchinobe 5-10-1, Sagamihara, Kanagawa 229-8558, Japan
(Received 21 May 2003; revised manuscript received 4 August 2003; published 15 December 2003)

Modulated structure of incommensurate composite crystal $(Sr_2Cu_2O_3)_{0.70}CuO_2$, "$Sr_{14}Cu_{24}O_{41}$," has been investigated by single-crystal x-ray-diffraction method using centrosymmetric $(3+1)$-dimensional superspace group. In $(Sr_2Cu_2O_3)_{0.70}CuO_2$, displacive modulation of O atom in the CuO_2 chain is fairly large. Considering the modulation of bond angles, it has been found that the Cu-O bond in the CuO_2 chain is tilting toward the Cu_2O_3 ladder in order that the O atom in the chain plays as apical oxygen for the CuO_4 square in the ladder. The bond-valence sum (BVS) method has been applied to investigate the hole distribution in the modulated structure of $(Sr_2Cu_2O_3)_{0.70}CuO_2$. It is indicated that the valence of Cu atom in the Cu_2O_3 ladder is $+2.04$, where about 0.03 holes are certainly transferred from the CuO_2 chain through the modulated O atom in the CuO_2. The BVS calculation has demonstrated that almost all of the holes are prepared in the CuO_2 chain by the large modulation of the Cu-O bond. Cu atoms in the modulated CuO_2 chain have been proved to form hole-ordered structure with next-nearest-neighbor Cu^{2+} ions separated by Cu^{3+} ion on the Zhang-Rice singlet site. The periodicity of the hole-ordered structure is five times of the average CuO_2 lattice along the crystallographic *c* axis, which is compatible with the spin-dimerized state at low temperature. The new model of the two-dimensional hole-ordered structure in the CuO_2 plane has been obtained by the BVS calculation. Furthermore, the two-dimensional configuration of the spin dimers has been successfully derived from the hole-ordered structure in the CuO_2 plane. It has been concluded that the valences of Cu atoms both in the Cu_2O_3 ladder and in the CuO_2 chain are well controlled by the modulated O atom in the CuO_2 chain.

DOI: 10.1103/PhysRevB.68.224108 PACS number(s): 74.72.Jt, 71.45.−d

I. INTRODUCTION

Since theoretical prediction that the $S=\frac{1}{2}$ one-dimensional antiferromagnetic Heisenberg chains should form a spin liquid state and have a spin gap in even-legged ladder structure was proposed,[1,2] much attention has been paid to so-called spin-ladder compounds. Especially the $Sr_{14-x}(Ca, La, Y)_xCu_{24}O_{41}$ series with two-legged Cu_2O_3 ladder and one-dimensional CuO_2 chain has been studied in detail by such measurement as resistivity, optical conductivity, magnetic susceptibility, neutron scattering, and NMR,[3] because there is another theoretical prediction that the spin-ladder compounds with even-numbered leg may show superconductivity under appropriate hole doping.[1,4] In the $Sr_{14-x}(Ca, La, Y)_xCu_{24}O_{41}$, $Sr_{14-x}Ca_xCu_{24}O_{41}$ series form a self-doped system, because the formal valence of Cu is $+2.25$. Substitution of Ca for Sr shows chemical pressure effect with lattice shrinkage and promotes hole transfer from the CuO_2 chain to the Cu_2O_3 ladder. At low temperature below 15 K, superconductivity has been attained under high pressure in the $Sr_{14-x}Ca_xCu_{24}O_{41}$ series such as $Sr_{2.5}Ca_{11.5}Cu_{24}O_{41}$ and $Sr_{0.4}Ca_{13.6}Cu_{24}O_{41}$.[5,6]

The ternary $Sr_{14}Cu_{24}O_{41}$ is well known as the parent material of the $Sr_{14-x}(Ca, La, Y)_xCu_{24}O_{41}$ series. In the crystallographic point of view, $Sr_{14}Cu_{24}O_{41}$ and $Sr_{14-x}(Ca, La, Y)_xCu_{24}O_{41}$ should be expressed as $(Sr_2Cu_2O_3)_{0.70}CuO_2$ and $(Sr_{2-x}(Ca, La, Y)_xCu_2O_3)_{0.70+\delta}CuO_2$, respectively, because they are called composite crystal with two interpenetrating layered substructures.[7] In $(Sr_2Cu_2O_3)_{0.70}CuO_2$, one of the substructures is the $Sr_2Cu_2O_3$ lattice and the other is the CuO_2 one. By x-ray structure analysis of average substructures, McCarron *et al.* have clarified that $(Sr_2Cu_2O_3)_{0.70}CuO_2$, "$Sr_{14}Cu_{24}O_{41}$," is composed of the Cu_2O_3 planes with two-legged ladders and the planes of edge-shared CuO_2 chains, alternately stacked.[8] In $(Sr_2Cu_2O_3)_{0.70}CuO_2$, the Cu_2O_3 ladders and the CuO_2 chains are separated by a sheet of Sr atoms in the $Sr_2Cu_2O_3$ substructure. The $Sr_2Cu_2O_3$ substructure and the CuO_2 substructure are mutually incommensurate because the ratio of the in-plane lattice constants of the average substructures along the leg of Cu_2O_3 ladder and the chain of the CuO_2 is irrational. Because of the mutual incommensurability, it can be expected that the structural modulations between the substructures occur.

Recently, Matsuda *et al.* have reported that the CuO_2 chain in $(Sr_2Cu_2O_3)_{0.70}CuO_2$ shows spin-gap behavior accompanied by the formation of spin-dimerized state at low temperature below 85 K.[9] After their unexpected finding, there have been arguments about the structure and the periodicity of the spin dimer in the CuO_2 chain in

$(Sr_2Cu_2O_3)_{0.70}CuO_2$.[10,11] It is worth noting that Takigawa *et al.*, by ^{63,65}Cu NMR/NQR measurements, have successfully distinguished magnetic Cu^{2+} ions from nonmagnetic Cu^{3+}, which form the so-called Zhang-Rice singlet.[12] They have indicated that the dimer with $\langle\uparrow(Cu^{2+})\rangle$-$\langle 0(Cu^{3+})\rangle$-$\langle\downarrow(Cu^{2+})\rangle$ spin fragment is formed in the CuO_2 chain in $(Sr_2Cu_2O_3)_{0.70}CuO_2$. By inelastic neutron-scattering method, Eccleston *et al.* have revealed that the spin dimer with $\langle\uparrow\rangle$-$\langle 0\rangle$-$\langle\downarrow\rangle$ has a periodicity of five units of the average structure of the CuO_2 chain.[13] On the basis of the periodicity of the spin dimer in one CuO_2 chain, Regnault *et al.* and Matsuda *et al.* have independently proposed the two-dimensional models of the magnetic ordering in the plane of the CuO_2 chains.[14,15] An essential difference between their models is the mode of relative arrangements of the $\langle\uparrow\rangle$-$\langle 0\rangle$-$\langle\downarrow\rangle$ dimers between neighboring CuO_2 chains. At present therefore the two-dimensional configuration of the spin dimers in the CuO_2 plane in $(Sr_2Cu_2O_3)_{0.70}CuO_2$ seems to be unsettled.

On the other hand, by means of electrical resistivity measurement, Carter *et al.* have suggested that charge-ordering behavior is caused by excess holes located on the CuO_2 chain in $(Sr_2Cu_2O_3)_{0.70}CuO_2$ around 250 K.[16] After their attractive work, there also have been controversies about the periodicity of hole-ordered structure. By using the x-ray diffraction method, Cox *et al.* have observed weak satellite reflections along 00*l* scan at 50 K. They claimed that the satellite reflections are brought about by the charge-ordering effect in the CuO_2 chain because the intensity of the satellites decreases with increasing temperature. Successively, Fukuda *et al.* also observed the satellites at low temperature. Cox *et al.* and Fukuda *et al.* have proposed that the periodic length of the hole-ordered CuO_2 chain along the crystallographic *c* axis is approximately four and five times, respectively, as long as that of the average CuO_2 lattice.[17,18] The apparent discrepancy between their results seems to come from the fact that the number of x-ray data with only 00*l* reflections is insufficient to refine the structure parameters of the CuO_2 chain. In both cases, the mutual lattice modulations between the Cu_2O_3 ladder and the CuO_2 chain have been ignored. Consequently, well-refined model of the hole-ordered structure including the effect of structural modulation in the CuO_2 chain has not been proposed at all. The more reliable model of the hole-ordered structure, which is indispensable for the spin-dimerization in the CuO_2 at low temperature, should be obtained from the modulated structure of $(Sr_2Cu_2O_3)_{0.70}CuO_2$.

The modulated structure of $(Sr_2Cu_2O_3)_{0.70}CuO_2$ is a quasiperiodic system with one-dimensional lattice modulations in both substructures. Therefore it can be closely described by the use of $(3+1)$-dimensional superspace-group symmetry.[19,20] In the conventional structure analysis by McCarron *et al.*,[8] however, the presumed centrosymmteric space groups, namely *Fmmm* for the $Sr_2Cu_2O_3$ substructure and *Amma* for the CuO_2 one, do not meet the condition of the symmetry of $(3+1)$-dimensional superspace groups well. In addition, after their structure refinement of the CuO_2 part, the *R* value was 0.129. The rather high *R* value suggests that the effect of lattice modulation on the CuO_2 chain is considerably large and should not be ignored in the structure analysis. Subsequently, Ukei *et al.* have reported the modulated structure analysis of $(Sr_2Cu_2O_3)_{0.70}CuO_2$ with the use of $(3+1)$-dimensional superspace-group symmetry.[21] In their modulated structure analysis, the acentric superspace group $A2_1ma(01\gamma)0s0$, for both substructures was employed. According to their results, the distances between Sr in the $Sr_2Cu_2O_3$ substructure and O in the CuO_2 substructure range from 1.95 to 2.87 Å [see Fig. 4(b)]. In their model with the acentric superspace group, the minimum distance between Sr and O in the CuO_2 chain is too short and the modulation amplitudes of the Sr-O distances are too large. Thus far there have been presented no models of the modulated structure of pure $(Sr_2Cu_2O_3)_{0.70}CuO_2$ that show the structural interaction between the substructures quite satisfactorily.

On the other side, Jensen *et al.* have demonstrated with impurities-mixed samples that the superspace group of $(Sr_{1.92}Bi_{0.08}Cu_2O_3)_{0.70}CuO_2$, "$Sr_{13.44}Bi_{0.56}Cu_{24}O_{41}$," is centrosymmetric, which is different from the acentric one of Ca-rich $(Sr_{0.057}Ca_{1.943}Cu_2O_3)_{0.70+\delta}CuO_2$, "$Sr_{0.4}Ca_{13.6}Cu_{24}O_{41}$."[22,23] According to Kato *et al.* and Matsuda *et al.*, more remarkable is that the spin gap in the CuO_2 chain in $(Sr_2Cu_2O_3)_{0.70}CuO_2$ is surprisingly depressed when a small amount of Y ion is substituted for Sr and disappear completely in $(Sr_{1.86}Y_{0.14}Cu_2O_3)_{0.70}CuO_2$.[24,25] Moreover, electrical resistivity in the Cu_2O_3 ladder part increases with the substituted Y ion.[10,26] These behaviors show that the properties of pure $(Sr_2Cu_2O_3)_{0.70}CuO_2$ are very sensitive to the impurities. This is also pointed out in the electronic phase diagram of the $[Sr_{2-x}(Ca, La, Y)_xCu_2O_3]_{0.70+\delta}CuO_2$, "$Sr_{14-x}(Ca, La, Y)_xCu_{24}O_{41}$" series.[27] In the impurity-substituted $(Sr_2Cu_2O_3)_{0.70}CuO_2$, considerable amounts of holes seem to be redistributed drastically accompanied by the change of the structural modulation. It seems easily realized that the structural modulation between the substructures and the resulting hole distribution are important factors in occurrence of the physical properties of $(Sr_2Cu_2O_3)_{0.70}CuO_2$. Actually, by optical measurement, it has been suggested that a small number of holes are possibly transferred between the substructures in the $(Sr_2Cu_2O_3)_{0.70}CuO_2$.[28]

Taking into account the introduction mentioned above, it is very important to investigate the modulated structure of pure $(Sr_2Cu_2O_3)_{0.70}CuO_2$, which is free from the chemical pressure effect with Ca doping, to understand the mechanism of the hole transfer and the hole distribution. The hole distribution in the modulated structure enables us to obtain more reliable model of the hole-ordered structure in the CuO_2 plane of $(Sr_2Cu_2O_3)_{0.70}CuO_2$. In particular, to see the effect of the structural modulation on the hole ordering, it is important to study the modulated structure of $(Sr_2Cu_2O_3)_{0.70}CuO_2$ at room temperature, where the charge-ordering effect is absent. Furthermore, the hole-ordered structure seems to give the clue to the spin-dimerized state of the CuO_2 chains. In the present work therefore we have investigated the symmetry and the modulated

structure of mutually incommensurate composite crystal, $(Sr_2Cu_2O_3)_{0.70}CuO_2$, "$Sr_{14}Cu_{24}O_{41}$," by the use of (3+1)-dimensional superspace group. The bond-valence sum (BVS) method considering the modulated composite structure has been applied to investigate the hole distribution, the hole-ordered structure, and the role of the atomic modulation in $(Sr_2Cu_2O_3)_{0.70}CuO_2$.

II. EXPERIMENT

Single composite crystals of $(Sr_2Cu_2O_3)_{0.70}CuO_2$ were grown by the traveling solvent floating zone (TSFZ) method. A single composite crystal of $(Sr_2Cu_2O_3)_{0.70}CuO_2$ with dimensions about $0.3\times0.2\times0.04$ mm^2 was used for the structure analysis. The composite diffraction patterns of $(Sr_2Cu_2O_3)_{0.70}CuO_2$ were identified by x-ray precession method with Mo$K\alpha$ radiation ($\lambda=0.71073$ Å). In the procedure of the camera technique, Imaging plate (BAS UR 5 $\times$5 in. type, Fuji Photo Film Co., Ltd.) was used to detect the weak satellite reflections of composite structure of $(Sr_2Cu_2O_3)_{0.70}CuO_2$. The x-ray-diffraction data of both substructures were collected together with common reflections at room temperature using a Rigaku AFC5 diffractometer (Mo$K\alpha$ radiation). The lattice constants of both average substructures were refined by least-squares method using 39 reflections including eight common ones in the range $27<2\theta<30°$. The lattice constants of orthorhombic average substructures of $(Sr_2Cu_2O_3)_{0.70}CuO_2$ were refined as $a=11.4794(8)$, $b=13.4060(10)$, and $c=3.9341(9)$ Å for the $Sr_2Cu_2O_3$ part and $a=11.4765(13)$, $b=13.4067(12)$, and $c=2.7519(19)$ Å for the CuO_2 one. These values are more accurate than those obtained by Ukei *et al.*,[21] which suggests that the quality of our sample is more appropriate for structure analysis. The composition of $(Sr_2Cu_2O_3)_{0.70}CuO_2$ was determined from the ratio of cell dimensions of each average substructure. In our data collections, 1346 reflections were measured by ω-2θ scan mode in the range $3<2\theta<60°$ and 448 unique reflections with $|F_o|>3\sigma(|F_o|)$ were considered to be observed ones. Lorentz polarization corrections and absorption corrections were applied to all of the collected reflections. All of the calculations for the structure refinement of the modulated $(Sr_2Cu_2O_3)_{0.70}CuO_2$ were carried out using a computer program system for the refinement of composite crystal structures, FMLSM.[29] In our calculations, neutral atomic scattering factors were taken from Cromer and Mann.[30] Anomalous dispersion factors used throughout this procedure are those given by Cromer and Lieberman.[31] The interatomic distances and bond angles were calculated by using the program for the analysis of chemical bonds, BONDL, in the FMLSM and the program to plot modulation functions, MODPLT, in a computer program for the refinement of modulated structures, REMOS.[20] The modulated structure of $(Sr_2Cu_2O_3)_{0.70}CuO_2$ was drawn by the use of the program for parallel and perspective projections of modulated structures, PRJMS, in the REMOS.

III. RESULTS AND DISCUSSION

A. Superspace-group description and structure refinement of $(Sr_2Cu_2O_3)_{0.70}CuO_2$

The lattice constants of the incommensurate basic structure of $(Sr_2Cu_2O_3)_{0.70}CuO_2$ are determined as $a=11.4794(8)$, $b=13.4060(10)$, $c_1=2.7519(19)$, and $c_2=3.9341(9)$ Å and the incommensurability between the average substructures are expressed as $\sigma=(0\,0\,\gamma)$ where $\gamma=c_2^*/c_1^*=c_1/c_2=0.699$. Therefore the accurate chemical composition of the so-called $Sr_{14}Cu_{24}O_{41}$ should be described from the detailed formula of $(Sr_2Cu_2O_3)_{0.70}CuO_2$ as $Sr_{14.0}Cu_{24}O_{41.0}$. The chemical composition of $Sr_{14}Cu_{24}O_{41}$ was discussed by Hiroi *et al.* by the use of electron diffraction method.[11] They have suggested that oxygen nonstoichiometry is possible in $Sr_{14}Cu_{24}O_{41}$ and expressed its chemical composition as $Sr_{14}Cu_{24}O_{41+\delta}$. Although they have estimated that the δ ranges from -0.7 to 0.9, positive values of δ is impossible from our view about the composite structure of $(Sr_2Cu_2O_3)_{0.70}CuO_2$. At least δ must be a negative, even if the oxygen nonstoichiometry occurs. However, such nonstoichiometry is not appreciated in our following modulated structure analysis.

The one-dimensionally modulated structure of composite crystal $(Sr_2Cu_2O_3)_{0.70}CuO_2$ can be described by the use of (3+1)-dimensional superspace group symmetry. The basis (s_1,s_2,s_3,s_4) of $(Sr_2Cu_2O_3)_{0.70}CuO_2$ in (3+1)-dimensional superspace are related to the basis $(a_\nu,b_\nu,c_\nu,d_\nu)$ of the νth substructure by the transformation P^ν as

$$(a_\nu,b_\nu,c_\nu,d_\nu)=(s_1,s_2,s_3,s_4)P^\nu, \tag{1}$$

where

$$P^1=\begin{pmatrix}1&0&0&0\\0&1&0&0\\0&0&1&0\\0&0&\gamma&1\end{pmatrix} \text{ and } P^2=\begin{pmatrix}1&0&0&0\\0&1&0&0\\0&0&1/\gamma&-(1/\gamma)\\0&0&1&0\end{pmatrix}. \tag{2}$$

The bases (a_ν,b_ν,c_ν) in $(a_\nu,b_\nu,c_\nu,d_\nu)$ are equivalent to those of average substructures in three-dimensional physical space.

If we take *A*-centered lattices in the orthorhombic system for both substructures, all of the x-ray reflections of $(Sr_2Cu_2O_3)_{0.70}CuO_2$ observed are indexed with four integer indices (*hklm*) as

$$H=ha^*+kb^*+lc_1^*+mc_2^*, \tag{3}$$

where the set of $\{hkl0\}$ corresponds to reflections from the CuO_2 substructure and the $\{hk0m\}$ are from the $Sr_2Cu_2O_3$ substructure. The former and the latter correspond to the satellite reflections with *l*th and *m*th order for the $Sr_2Cu_2O_3$ substructure and the CuO_2 substructure, respectively. The $\{hk00\}$ is common reflections which precisely prove that $(Sr_2Cu_2O_3)_{0.70}CuO_2$ forms a composite crystal structure. The $\{hklm\}$ with $lm\neq0$ is the intrinsic satellite reflections indicating the mutual lattice modulations between the sub-

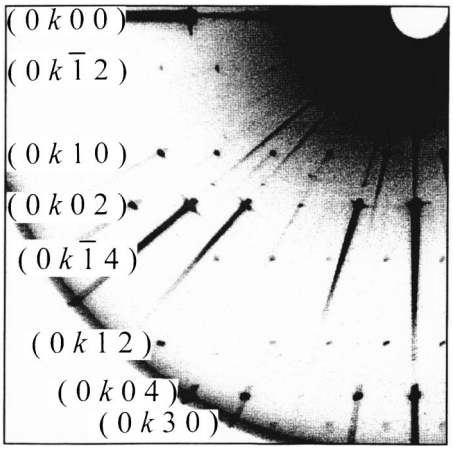

FIG. 1. The composite $0klm$ diffraction pattern of $(Sr_2Cu_2O_3)_{0.70}CuO_2$, "$Sr_{14}Cu_{24}O_{41}$," observed by x-ray photograph.

structures. The reflection conditions of acentric $A2_1ma(01\gamma)0s0$ assumed for $(Sr_2Cu_2O_3)_{0.70}CuO_2$ by Ukei *et al.* are $k+l+m=2n$ for $hklm$ and $m=2n$ for $h0lm$. In addition, as the x-ray precession photograph of $(Sr_2Cu_2O_3)_{0.70}CuO_2$ in Fig. 1 shows, we have observed another condition for the satellite $0klm$ as $m=2n$. This leads to the centrosymmetric superspace groups for both substructures of $(Sr_2Cu_2O_3)_{0.70}CuO_2$ as $Amma(01\gamma)ss0$ for the CuO_2 part and $Acca(01\gamma)$ for the $Sr_2Cu_2O_3$ part where *Acca* is obtained from *Abma* by shifting the origin as $(0\ \frac{1}{4}\ \frac{1}{4})$. The convergent beam electron diffraction (CBED) method has also clarified the presence of center of symmetry for both substructures.[32] The CBED observation has shown that the point-group symmetry of both average substructures is not $2mm$ but mmm. Thus the generators of the symmetry operations of the superspace groups employed are $(\sigma_1|\frac{1}{2},0,0,\frac{1}{2})$, $(\sigma_2|0,0,0,\frac{1}{2})$, $(I|0,0,0,0)$, and $(E|0,\frac{1}{2},\frac{1}{2},\frac{1}{2})$. The symmetry operations for superspace groups of $(Sr_2Cu_2O_3)_{0.70}CuO_2$ have turned out to be equivalent to those for $Amma(001+\gamma)ss$-1 of Bi-doped $(Sr_{1.92}Bi_{0.08}Cu_2O_3)_{0.70}CuO_2$.[22] As Kato *et al.* and Matsuda *et al.* claimed, we must be reminded that even a small amount of trivalent ion substituted for Sr in the $Sr_2Cu_2O_3$ substructure greatly affect the structural feature and charge distribution of pure $(Sr_2Cu_2O_3)_{0.70}CuO_2$.[24,25] Here, we can predict that the symmetry of $(Sr_2Cu_2O_3)_{0.70}CuO_2$ is unchanged by substituting a small amount of Bi, Y, or La for Sr. It should be also emphasized that the structural modulations of $(Sr_2Cu_2O_3)_{0.70}CuO_2$, "$Sr_{14}Cu_{24}O_{41}$," are quite different from those of the Ca-rich compounds such as $(Sr_{0.057}Ca_{1.943}Cu_2O_3)_{0.70+\delta}CuO_2$, "$Sr_{0.4}Ca_{13.6}Cu_{24}O_{41}$."[23] Distinct from the centrosymmetric superspace groups for the substructures in $(Sr_2Cu_2O_3)_{0.70}CuO_2$, the acentric superspace groups $F222(11\gamma)$ are employed for both substructures in $(Sr_{0.057}Ca_{1.943}Cu_2O_3)_{0.70+\delta}CuO_2$.

In the modulated structure analysis, each atomic position (x_ν, y_ν, z_ν, t) in the νth substructure are obtained from the coordinate (u_1, u_2, u_3, u_4) of four-dimensional structure in $(3+1)$-dimensional superspace as

$$(x_\nu, y_\nu, z_\nu, t)=(u_1, u_2, u_3, u_4)[(P^\nu)^{-1}]^T, \quad (4)$$

where t is the internal parameter in $(3+1)$-dimensional superspace.

The modulated composite structure of $(Sr_2Cu_2O_3)_{0.70}CuO_2$ was refined with 448 unique data. At first, unmodulated incommensurate basic structure was refined with isotropic temperature factors for all atoms. At this stage, R and R_w values are 0.102 and 0.105, respectively and $B_{iso.}$ of O(1) atom in the CuO_2 chain is 2.61 Å^2, which is rather larger than those of O(2) ($B_{iso.}=0.45$ Å^2) and O(3) ($B_{iso.}=0.75$ Å^2) in the Cu_2O_3 ladder. The large value of $B_{iso.}$ of O(1) suggests that displacive modulation of O(1) atom is fairly large in the CuO_2 chain. In the second step, we have adopted the structure model with first-order waves of the displacive modulation for all atomic positions. With harmonic modulation function, the atomic position in the νth substructure is expressed as

$$(x_\nu, y_\nu, z_\nu, t)=\mathbf{r}_{\nu 0}+\Sigma\{a_k \cos[2\pi\mathbf{k}P^\nu(\mathbf{r}_{\nu 0},t)^T] + b_k \sin[2\pi\mathbf{k}P^\nu(\mathbf{r}_{\nu 0},t)^T]\}, \quad (5)$$

where $\mathbf{r}_{\nu 0}=(x_\nu, y_\nu, z_\nu)_0$ is the atomic position of the νth average structure and $\mathbf{k}$ is the modulation wave vectors. The refinement converged to an R value of 0.058 and an R_w value of 0.069, where anisotropic temperature factors were used for the atoms other than O(2). At this stage, the equivalent thermal parameter $B_{eq.}$ of O(1) was 1.45 Å^2. In the final step of the structure refinement, the effect of the second order of all of the atomic modulation functions was checked. It has been revealed that the second-order modulations for Sr in the $Sr_2Cu_2O_3$ and O(1) in the CuO_2 are significant in our final model of the modulated structure of $(Sr_2Cu_2O_3)_{0.70}CuO_2$. The refined atomic parameters are listed in Table I, where the R value converged to 0.054 and the R_w value was 0.067. The statistical value of AIC (akaike information criterion) was 2702.[33] In Table I, several Fourier coefficients of the modulation function are fixed at 0 by considering the site symmetry of each atom in the average substructures. The thermal parameters are presented by $U_{eq.}$ which is equivalent to $B_{eq.}/8\pi^2$. It should noted that the thermal parameter $B_{eq.}$ of O(1) has been reduced to 1.03 Å^2 in the modulated structure. As we can see from Table I, the number of independent atoms has been decreased from nine in the acentric model to six in our centrosymmetric structure.

B. Modulated structure of $(Sr_2Cu_2O_3)_{0.70}CuO_2$

With the atomic parameters listed in Table I, the modulated structure of $(Sr_2Cu_2O_3)_{0.70}CuO_2$ is drawn in Fig. 2. In Fig. 3, the displacements of all of the independent atoms along each crystallographic axis are calculated in the internal t space in $(3+1)$-dimensional superspace. Here we must note that the displacement of Cu(1) in the CuO_2 substructure are absent because the first order of the displacive modulation for Cu(1) is fixed at 0 by the symmetrical constraint. In our refinement, the second order of the modulation has not been adopted for Cu(1) because it has brought about no improvements in the values of R, R_w, and AIC. On the whole,

TABLE I. Atomic parameters of the modulated structure of $(Sr_2Cu_2O_3)_{0.699}CuO_2$ "$Sr_{14}Cu_{24}O_{41}$" with estimated standard deviations in parentheses. Average positions and modulation amplitudes are represented by fractional coordinates and Å, respectively. The structure is refined in the superspace group symmetry $Amma(01\gamma)ss0$: $Acca(01\gamma)$. The modulation parameters a_k and b_k are the cosine and sine amplitudes of the Fourier series of the modulation function, where k is the modulation vector.

Atom	Occupancy	x	y	z	$100(U_{eq.})$
Cu(1)					
Average	0.25	0.25	0.5	0.373(1)	1.26(8)
a_{0001}	0.0	0.0	0.0	0.0	0.0
b_{0001}	0.0	0.0	0.0	0.0	0.0
O(1)					
Average	0.5	0.138(1)	0.5	0.878(7)	1.3(7)
a_{0001}	0.0	0.0	−0.08(8)	0.0	0.0
b_{0001}	0.0	0.0	−0.29(2)	0.0	0.0
a_{0002}	0.0	−0.01(4)	0.0	0.14(11)	0.0
b_{0002}	0.0	−0.08(6)	0.0	−0.06(2)	0.0
Sr					
Average	0.5	0.5	0.3785(1)	0.25	0.79(6)
a_{0010}	0.0	0.0	−0.040(6)	0.0	0.0
b_{0010}	0.0	−0.028(6)	0.0	0.106(7)	0.0
a_{0020}	0.0	0.0	−0.05(2)	0.0	0.0
b_{0020}	0.0	−0.024(6)	0.0	0.000(11)	0.0
Cu(2)					
Average	0.5	0.3344(2)	0.25	0.744(4)	0.70(8)
a_{0010}	0.0	0.0	−0.021(12)	0.0	0.0
b_{0010}	0.0	0.0	−0.055(12)	0.0	0.0
O(2)					
Average	0.5	0.169(1)	0.25	0.76(1)	0.1(3)[a]
a_{0010}	0.0	0.0	−0.12(5)	0.0	0.0
b_{0010}	0.0	0.0	0.11(5)	0.0	0.0
O(3)					
Average	0.25	0.5	0.25	0.75	0.7(7)
a_{0010}	0.0	0.0	−0.12(5)	0.0	0.0
b_{0010}	0.0	0.0	0.0	0.0	0.0

[a]Isotropic temperature factor.

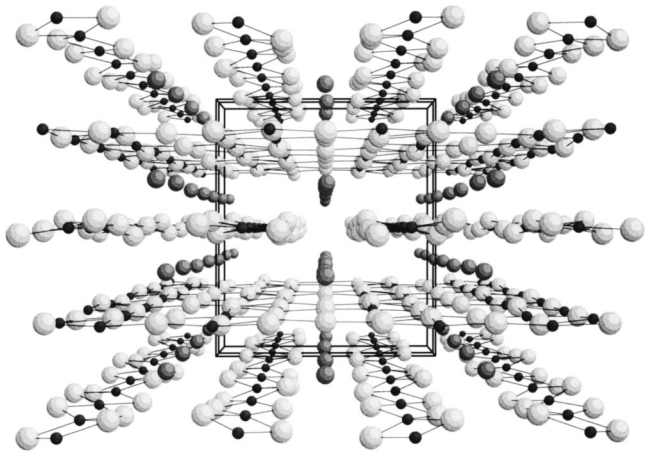

FIG. 2. Mutually incommensurate modulated structure of $(Sr_2Cu_2O_3)_{0.70}CuO_2$, "$Sr_{14}Cu_{24}O_{41}$." Small solid circles denote Cu atoms; medium (dark gray-colored) circles represent Sr atoms; large (light gray-colored) circles are O atoms.

as we can see from Fig. 3, the modulation amplitude becomes large along the *a*, *c*, and *b* axis in that order. The modulation amplitudes along the *a* axis are slight, because both average substructures have equivalent lattice dimension and do not interpenetrate with each other along the *a* axis. The amplitudes along the *c* axis are larger, because the CuO_2 substructure and the $Sr_2Cu_2O_3$ substructure are mutually incommensurate along the *c* axis. Since the mutually incommensurate substructures are stacked alternately along the *b* axis, the modulation amplitudes along the *b* axis are most important. We can confirm that these features are also valid in the Bi-doped $(Sr_{1.92}Bi_{0.08}Cu_2O_3)_{0.70}CuO_2$.[22] However, the differences of the atomic modulation amplitude between $(Sr_2Cu_2O_3)_{0.70}CuO_2$ and $(Sr_{1.92}Bi_{0.08}Cu_2O_3)_{0.70}CuO_2$ are appreciable for O atoms. In particular, the difference of the modulation amplitude of the O atom in the CuO_2 chain is estimated to be more than 0.05 Å in all axes. Thus the significant difference in the mode of the modulation of the O atom seems to affect the distribution of holes in the CuO_2 chain which control the physical properties of $(Sr_2Cu_2O_3)_{0.70}CuO_2$.[10,24–27]

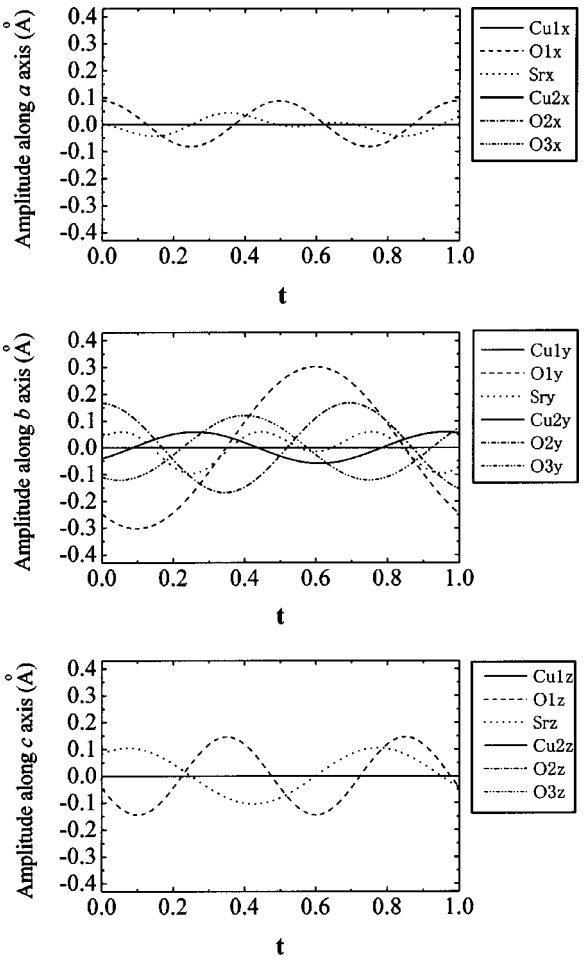

FIG. 3. Displacive modulation amplitudes of independent atoms in $(Sr_2Cu_2O_3)_{0.70}CuO_2$, "$Sr_{14}Cu_{24}O_{41}$." The t is the internal coordinate in $(3+1)$-dimensional superspace.

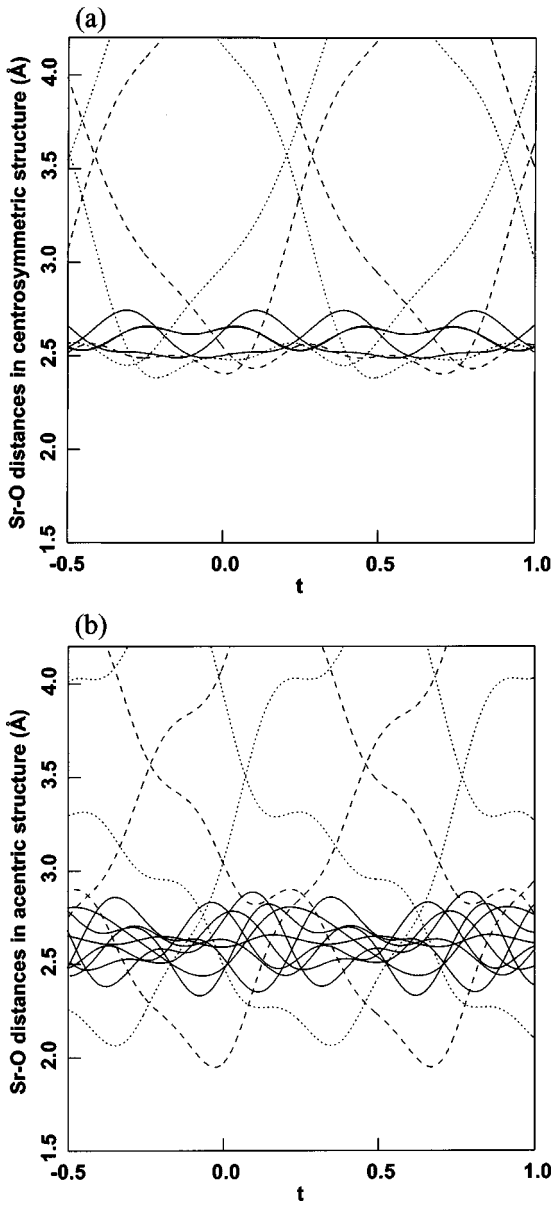

FIG. 4. Sr-O distances in the modulated structure of $(Sr_2Cu_2O_3)_{0.70}CuO_2$ with centrosymmetric (a) and acentric (b) superspace groups. The solid lines denote Sr-O distances in the $Sr_2Cu_2O_3$ substructure; the dotted and dashed lines represent Sr-O distances between the $Sr_2Cu_2O_3$ substructure and the CuO_2 substructure.

As for the elements in $(Sr_2Cu_2O_3)_{0.70}CuO_2$, the displacive modulations of Cu, Sr, and O become large in that order. Besides the modulation of O atoms, the modulation of the Sr atom is large enough and effective for the stacking of both substructures. The bond formation between the Sr atom and O atoms in the Cu_2O_3 ladder and the CuO_2 chain seems to be indispensable in stabilizing the modulated composite structure of $(Sr_2Cu_2O_3)_{0.70}CuO_2$, because the sheet of the Sr atom is situated between the planes of the Cu_2O_3 ladder and the CuO_2 chain. Thus to reveal the structural stability of the modulated $(Sr_2Cu_2O_3)_{0.70}CuO_2$, we have calculated all of the Sr-O lengths for both centrosymmetric and acentric models in Figs. 4(a) and (b), respectively. The interatomic distances between Sr and O(1) in the CuO_2 calculated with our centrosymmetric superspace groups, that is, $Amma(01\gamma)ss0$ for the CuO_2 substructure and $Acca(01\gamma)$ for the $Sr_2Cu_2O_3$ substructure, range from 2.40(5) Å at $t=0.49$ to 2.57(5) Å at $t=0.28$, where t is expressed as $t=-\gamma u_3+u_4$. They should be compared with those of the structure model with acentric superspace group, $A2_1ma(01\gamma)0s0$, which was proposed by Ukei *et al.* According to their results,[21] the interatomic distances between Sr and O in the CuO_2 range from 1.95 to 2.87 Å, and hence their modulation amplitudes are much larger than those of our results. As we can see from the present comparison, the smaller amplitude of the bondings at the interface between the substructures should be obtained in a more stable and appropriate structure model. Moreover, modulation amplitudes of the Sr-O lengths in the $Sr_2Cu_2O_3$ in the centrosymmetric model are smaller than those in the acentric one. In our model, as a result, all of the Sr-O lengths show appropriate values and their modulation amplitudes are suppressed less than about 0.3 Å.

In Fig. 5, Cu-O bonds in the Cu_2O_3 ladder in $(Sr_2Cu_2O_3)_{0.70}CuO_2$ are illustrated. All of the modulation amplitudes of the Cu-O bonds in the Cu_2O_3 ladder are less

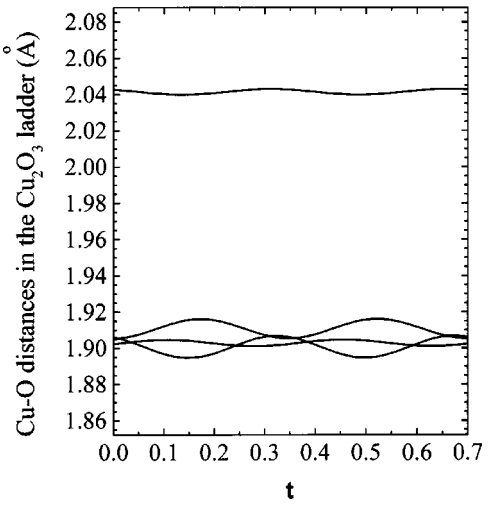

FIG. 5. Cu-O distances in the Cu_2O_3 ladder in $(Sr_2Cu_2O_3)_{0.70}CuO_2$.

than 0.02 Å. Compared with the weak modulation in the Cu_2O_3 ladder in $(Sr_2Cu_2O_3)_{0.70}CuO_2$, the magnitudes of the modulation in the Cu_2O_3 ladder in Ca-rich $(Sr_{2-x}Ca_xCu_2O_3)_{0.70+\delta}CuO_2$ compounds are appreciable. From the preliminary results using the polycrystalline sample, the maximum modulation amplitude of the Cu-O bonds in the Cu_2O_3 ladder in $(Sr_{0.057}Ca_{1.943}Cu_2O_3)_{0.70+\delta}CuO_2$, "$Sr_{0.4}Ca_{13.6}Cu_{24}O_{41}$," amounts to about 0.1 Å.[23] Thus in the $(Sr_{2-x}Ca_xCu_2O_3)_{0.70+\delta}CuO_2$ series, we can expect that the effect of structural modulation on the Cu_2O_3 ladder becomes weak with decreasing the substitution of the Ca atom for the Sr atom. It should be noted that all of the atomic displacements in the Cu_2O_3 in $(Sr_2Cu_2O_3)_{0.70}CuO_2$ are confined along the stacking direction, because the *x* and *z* elements of the modulation functions for Cu(2), O(2), and O(3) are fixed at 0 by the symmetrical constraint (see Table I and Fig. 3). To evaluate the flatness of the two-legged Cu_2O_3 ladder in $(Sr_2Cu_2O_3)_{0.70}CuO_2$, then, the angles between *ac* plane and the selected bonds in the Cu_2O_3 ladder are calculated. As we can see from Table II, the two-legged ladder bends less than about 4° along the *c* axis, while the alignment of the $[Cu(2)O(2)]_2$ square between the two-legged ladders is slightly rugged. With these structural features, the Cu_2O_3 ladder in $(Sr_2Cu_2O_3)_{0.70}CuO_2$ forms a low-dimensional electron system, where a charge-density wave develops in the ladder below 250 K.[34]

In contrast to the Cu_2O_3 ladder, the effect of structural modulation on the CuO_2 chain is enormous in $(Sr_2Cu_2O_3)_{0.70}CuO_2$ (see Fig. 2). The occurrence of the large modulation in the CuO_2 chain seems a common feature in the $(Sr_{2-x}Ca_xCu_2O_3)_{0.70+\delta}CuO_2$, "$Sr_{14-x}Ca_xCu_{24}O_{41}$," series. In the Ca rich compounds such as $(Sr_{0.057}Ca_{1.943}Cu_2O_3)_{0.70+\delta}CuO_2$,[23] both Cu and O atoms in the CuO_2 modulate independently. However, in $(Sr_2Cu_2O_3)_{0.70}CuO_2$, only the O atom is modulated in the CuO_2 chain and the displacement of Cu is fixed at 0 by the symmetrical reason as mentioned before. We must realize that the site symmetries of Cu and O atoms in the *A*-centered CuO_2 in $(Sr_2Cu_2O_3)_{0.70}CuO_2$ with centrosymmetric superspace groups are quite different from those in the *F*-centered CuO_2 in $(Sr_{0.057}Ca_{1.943}Cu_2O_3)_{0.70+\delta}CuO_2$ with acentric superspace groups.

On account of the large thermal factor $B_{iso.}(=2.61\ Å^2)$ of O(1) in the average structure of $(Sr_2Cu_2O_3)_{0.70}CuO_2$, the modulation of O atom in the CuO_2 chain was presumed to be fairly large. By applying the modulation functions in Eq. (5) to the average substructure of the CuO_2, the reliability factors have been successfully reduced from $R/R_w = 0.157/0.194$ to $R/R_w = 0.066/0.076$ with $hkl0$ $(l \neq 0)$ reflections. The modulated Cu-O bonds in the CuO_2 chain in $(Sr_2Cu_2O_3)_{0.70}CuO_2$ are calculated in Fig. 6. In the CuO_2 chain, the Cu(1;*x*, *y*, *z*)-O(1;*x*, *y*, *z*) bond varies from 1.82(8) Å at $t=0.147$ to 2.00(8) Å at $t=0.389$ and the Cu(1;*x*, *y*, *z*)-O(1;*x*, *y*, $z-1$) bond varies from 1.74(7) Å at $t=0.019$ to 2.03(7) Å at $t=0.272$. The maximum modulation amplitude of the Cu-O bonds in the CuO_2 chain thus amounts to about 0.3 Å, which is considerably larger than the amplitude about 0.02 Å obtained for the Cu-O bonds in the Cu_2O_3 ladder. Because of the large amplitude of the Cu-O bonds caused by the modulated O(1) atom, hole modulation is expected to occur in the CuO_2 chain. In Fig. 7, the bond angles of O-Cu-O and Cu-O-Cu in the

TABLE II. The minimum and maximum values of the angles (deg.) between *ac* plane and the selected bonds in the Cu_2O_3 ladder in $(Sr_2Cu_2O_3)_{0.70}CuO_2$ with estimated standard deviations in parentheses. Corresponding *t* value in (3+1)-dimensional superspace is also presented.

Atoms and symmetry codes	Minimum	*t* value	Maximum	*t* value
Along the leg within two-legged ladder				
Cu(2;*x*, *y*, *z*)-O(2;$-x+\frac{1}{2}$, *y*, $z+\frac{1}{2}$)	1.0(6)	0.13	3.3(9)	0.31
Cu(2;*x*, *y*, *z*)-Cu(2;*x*, *y*, $z+1$)	0.0(12)	0.06	1.7(4)	0.24
Along the rung within two-legged ladder				
Cu(2; *x*, *y*, *z*)-O(3;*x*, *y*, *z*)	0.7(5)	0.28	3.6(13)	0.11
Cu(2;*x*, *y*, *z*)-Cu(2;$x+1$, *y*, *z*)	0.7(5)	0.05	1.8(4)	0.23
Between two-legged ladders				
Cu(2;*x*, *y*, *z*)-O(2;*x*, *y*, *z*)	2.2(15)	0.00	6.4(15)	0.17

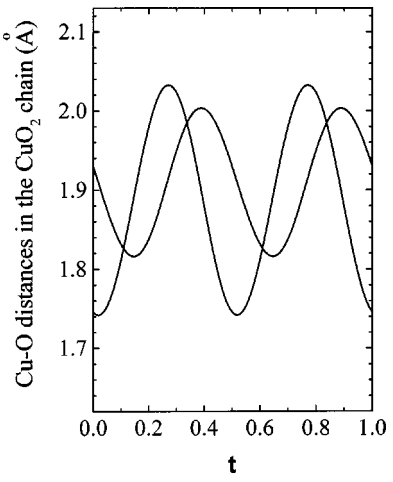

FIG. 6. Cu-O distances in the CuO_2 chain in $(Sr_2Cu_2O_3)_{0.70}CuO_2$.

CuO_2 chain are calculated. Along the *c* axis, the $O(1;x, y, z)$-$Cu(1;x, y, z)$-$O(1;x, y, z-1)$ angle varies from 86.9° at $t=0.07$ to 100.4° at $t=0.32$ and the $Cu(1;x, y, z)$-$O(1;x, y, z)$-$Cu(1;x, y, z+1)$ angle varies from 89.4° at $t=0.02$ to 96.6° at $t=0.26$. On account of the large displacement of O(1) atom, the modulation of the O-Cu-O bond angle is larger than that of the Cu-O-Cu angle. As we can see from Fig. 7, the Cu-O-Cu angle is mostly under 96°. Mizuno *et al.* theoretically predicted that the exchange interaction between the nearest-neighbor Cu^{2+} ions in the edge shared CuO_2 chain turns out to be ferromagnetic if the Cu-O-Cu angle is below about 95°.[35] Thus if the nearest-neighbor Cu^{2+} ions existed in all over the CuO_2 chain, ferromagnetic features could be observed at low temperature in $(Sr_2Cu_2O_3)_{0.70}CuO_2$.

C. Hole distribution in the modulated $(Sr_2Cu_2O_3)_{0.70}CuO_2$

From the chemical composition of $(Sr_2Cu_2O_3)_{0.70}CuO_2$, it is evident that the formal valence of Cu atom is +2.25 and

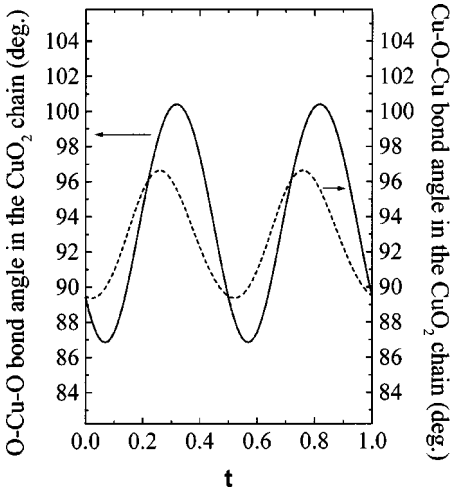

FIG. 7. O-Cu-O and Cu-O-Cu bond angles in the CuO_2 chain in $(Sr_2Cu_2O_3)_{0.70}CuO_2$.

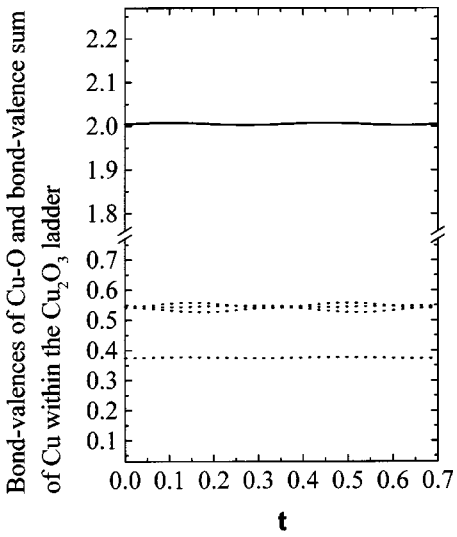

FIG. 8. Bond valences of Cu-O (dotted lines) and bond-valence sum (solid line) of Cu within the Cu_2O_3 ladder in $(Sr_2Cu_2O_3)_{0.70}CuO_2$.

that holes are self-doped in $(Sr_2Cu_2O_3)_{0.70}CuO_2$. From the modulated composite structure analysis in the present study, ununiform distribution of holes are expected in $(Sr_2Cu_2O_3)_{0.70}CuO_2$. Since Cu sites in $(Sr_2Cu_2O_3)_{0.70}CuO_2$ are nonequivalent with each other, bond-valence sum (BVS) calculation is one of the most effective methods to estimate local valences of Cu atoms.[36,37] By the BVS calculation with the average substructures of $(Sr_2Cu_2O_3)_{0.70}CuO_2$, Kato *et al.* attempted to estimate the mean valence of Cu atom in each substructure.[38] However, to understand the charge transfer between the substructures and the effect of lattice modulation exactly, we need to calculate the bond valences of the modulated Cu-O bonds in $(Sr_2Cu_2O_3)_{0.70}CuO_2$. In the case of the modulated structure of composite crystal, the BVS of the *i*th atom in the μth substructure $V_{i\mu}(t)$ is described as

$$V_{i\mu}(t)=\Sigma_j s_{i\mu,j\nu}(t)=\Sigma_j\Sigma_g \exp[\{r_0-r_{i\mu,j\nu}(t,g)\}/B], \tag{6}$$

where $s_{i\mu,j\nu}(t)$ and $r_{i\mu,j\nu}(t,g)$ are the bond valence and the interatomic distance between the *i*th atom in the μth substructure and the *j*th atom in the νth substructure, respectively. The *g* is the symmetry operation of the *j*th atom in $(3+1)$-dimensional superspace. The constant *B* is set as 0.37 and the parameter r_0 of the *i*th atom depends on its valence. The r_0 of Cu^{2+} selected from reference by Brown *et al.* is 1.679.[39]

By taking into account the four Cu-O bonds within the Cu_2O_3 ladder, the BVS of Cu(2) is calculated in the *t* space, as illustrated in Fig. 8. Because of the small modulation amplitudes of the Cu-O lengths, the BVS of Cu(2) is quite uniform in the ladder. The average BVS value of Cu(2) is 2.01, and accordingly Cu(2) seems to be almost undoped within the ladder plane of the Cu_2O_3. The angle-resolved photoemission spectroscopy (ARPES) experiment has also indicated that the Cu atom in the Cu_2O_3 ladder is substantially undoped.[40] By neglecting the structural modulation, the elec-

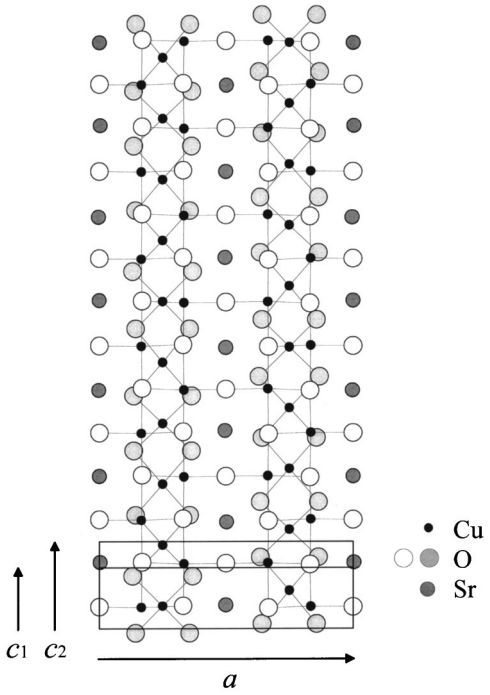

FIG. 9. Modulated composite structure of $(Sr_2Cu_2O_3)_{0.70}CuO_2$ along the *b* axis.

tronic structure calculation with local-density approximation method has obtained that the valence of Cu(2) in the ladder is 1.97.[41] On the whole, these quite similar results suggest that the weak modulation developed within the ladder plane hardly affects the electronic structure of the Cu_2O_3 ladder and prepares no holes in the Cu_2O_3 in $(Sr_2Cu_2O_3)_{0.70}CuO_2$. It should be kept in mind that, in the Ca-rich compound $(Sr_{0.057}Ca_{1.943}Cu_2O_3)_{0.70+\delta}CuO_2$, about 0.2 holes per Cu atom in the ladder are transferred from the CuO_2 chain.[42] Therefore in the absence of lattice shrinkage which is caused by chemical pressure effect with Ca doping, it seems much interesting to see whether structural modulation of the CuO_2 chain can cause hole doping to the Cu_2O_3 ladder or not in $(Sr_2Cu_2O_3)_{0.70}CuO_2$. Accordingly, we need to investigate the effect of the modulation of the O atom in the CuO_2 chain on the Cu_2O_3 ladder. We can see from Fig. 9 that the O(1) in the CuO_2 chain in $(Sr_2Cu_2O_3)_{0.70}CuO_2$ is, as in the case of $(Sr_{0.057}Ca_{1.943}Cu_2O_3)_{0.70+\delta}CuO_2$, aligned just above and below the Cu-O legs in the ladder even though the relative arrangement of neighboring CuO_2 chains in the *ac* plane is different to that of the Ca-rich compounds. Figure 10 shows selected Cu-O distances between the substructures in modulated $(Sr_2Cu_2O_3)_{0.70}CuO_2$. Evidently, the bonding between Cu(2) in the Cu_2O_3 ladder and O(1) in the CuO_2 chain seems most important between the substructures. The minimum of the Cu(2)-O(1) distance is 3.05(3) Å at $t=0.155$. To reveal the role of the modulated O atom in the CuO_2 chain exactly, the tilt angle of Cu(1)-O(1) bond are calculated together with the Cu(2)-O(1) distance. It can be seen from Fig. 11 that the Cu(2)-O(1) distance is attained to its minimum by the large tilt of the Cu(1)-O(1) bond from the *ac* plane. The minimum Cu(2)-O(1) distance should be compared to that of the corresponding Cu-O distance in

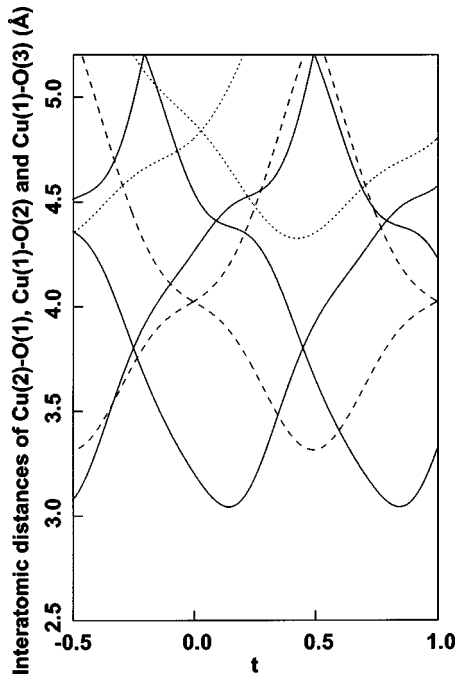

FIG. 10. Interatomic distances of Cu-O between the substructures. The solid lines denote distances between Cu(2) in the Cu_2O_3 and O(1) in the CuO_2; the dashed lines represent distances between Cu(1) in the CuO_2 and O(2) in the leg of the Cu_2O_3; the dotted lines are distances between Cu(1) in the CuO_2 and O(3) in the rung of the Cu_2O_3.

$(Sr_{0.057}Ca_{1.943}Cu_2O_3)_{0.70+\delta}CuO_2$.[23] With the lattice shrinkage by the chemical pressure effect, the minimum Cu-O distance between the substructures is about 2.68 Å in $(Sr_{0.057}Ca_{1.943}Cu_2O_3)_{0.70+\delta}CuO_2$, where the O atom in the CuO_2 chain is regarded as an apical atom for the CuO_4

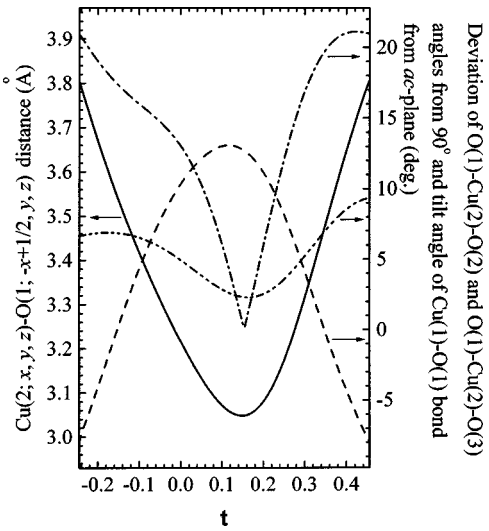

FIG. 11. Modulated interaction between the Cu_2O_3 ladder and the CuO_2 chain. The solid line denotes Cu(2)-O(1) distance between the substructures; the dashed-and-dotted and dashed-and-two-dotted lines represent deviation from 90° of O(1)-Cu(2)-O(2) and O(1)-Cu(2)-O(3) angles, respectively; the dashed line is the tilt angle of Cu(1)-O(1) bond from the *ac* plane.

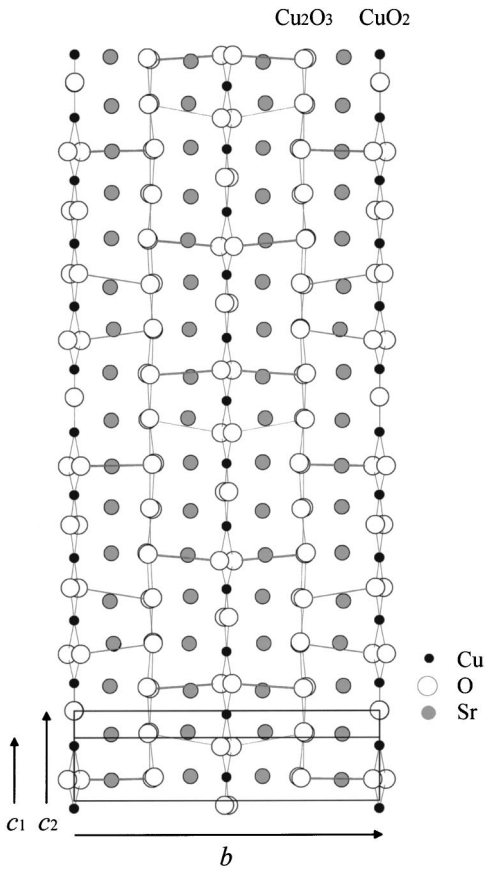

FIG. 12. Modulated composite structure of $(Sr_2Cu_2O_3)_{0.70}CuO_2$ along the *a* axis. The thin, medium, and wide gray-colored lines show the distances of Cu(2)-O(1) bondings less than 3.30, 3.20, and 3.10 Å, respectively.

square in the Cu_2O_3 ladder. Thus some apical O atoms in the CuO_2 and the CuO_4 squares form the elongated CuO_5 tetragonal pyramids on the ladder plane in $(Sr_{0.057}Ca_{1.943}Cu_2O_3)_{0.70+\delta}CuO_2$. In $(Sr_2Cu_2O_3)_{0.70}CuO_2$, on the other hand, to see if the O(1) atom in the CuO_2 chain really behaves like an apical atom for the CuO_4 square in the Cu_2O_3 ladder, O(1)-Cu(2)-O(2) and O(1)-Cu(2)-O(3) angles are evaluated. When the O(1)-Cu(2)-O(2) and the O(1)-Cu(2)-O(3) angles are close to 90°, the distortion of the elongated CuO_5 tetragonal pyramid should be small along the leg and the rung, respectively, in the ladder. As we can see from Fig. 11, the deviations of the O(1)-Cu(2)-O(2) and the O(1)-Cu(2)-O(3) angles from 90° tend to decrease as the Cu(2)-O(1) distance approaches its minimum. The marked correlation among the Cu(2)-O(1) distance and the O(1)-Cu(2)-O(2) and the O(1)-Cu(2)-O(3) angles around $t=0.15$ convince us that the O atom in the CuO_2 chain can be regarded as the apical atom for the CuO_4 squares in the Cu_2O_3 ladder and that holes can be transferred from the CuO_2 to the Cu_2O_3 in $(Sr_2Cu_2O_3)_{0.70}CuO_2$ (see Fig. 12). To evaluate the amounts of holes transferred from the CuO_2 chain to the Cu_2O_3 ladder, the BVS of the Cu(2)-O(1) bondings in the modulated structure of $(Sr_2Cu_2O_3)_{0.70}CuO_2$ was calculated. As we can see from Fig. 13, about 0.03 holes per Cu(2) atom are transferred from the CuO_2 chain to the Cu_2O_3 ladder. The hole

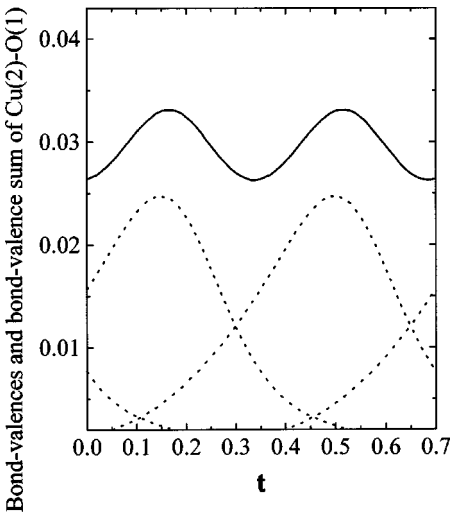

FIG. 13. Bond valences (dotted lines) and bond-valence sum (solid line) between Cu(2) in the Cu_2O_3 ladder and O(1) in the CuO_2 in $(Sr_2Cu_2O_3)_{0.70}CuO_2$.

transfer in $(Sr_2Cu_2O_3)_{0.70}CuO_2$ has been also indicated by optical conductivity measurement and polarization-dependent x-ray absorption spectrum.[28,43] Thus from the modulated structure analysis of $(Sr_2Cu_2O_3)_{0.70}CuO_2$, we have closely revealed that a finite number of holes are undoubtedly transferred, even in the absence of the chemical pressure effect with Ca doping, from the CuO_2 chain to the Cu atom in the Cu_2O_3 ladder through the modulated O atom in the CuO_2.

By considering the valence of Cu(2) in the ladder and the chemical composition of $(Sr_2Cu_2O_3)_{0.70}CuO_2$, most of the holes should be located in the CuO_2 chain. This is qualitatively consistent with the results from the ARPES experiment, optical conductivity measurement, and electronic structure calculation.[28,40,41] The average valence of Cu(1) atom in the CuO_2 chain is about 2.6. This shows that, in the $[Sr_{2-x}(Ca, La, Y)_xCu_2O_3]_{0.70+\delta}CuO_2$ series, the maximum amounts of holes are prepared in the CuO_2 chain in $(Sr_2Cu_2O_3)_{0.70}CuO_2$. Thus the BVS method was also applied to reveal the hole distribution in the modulated CuO_2 chain in $(Sr_2Cu_2O_3)_{0.70}CuO_2$. If we adopt 1.73 as the r_0 of Cu^{3+} in the BVS calculation,[37] the r_0 of the Cu(1) atom is obtained by interpolation to be 1.71. Taking into account the modulated Cu-O bonds in the CuO_2 chain, the bond valences and the BVS of Cu(1) are calculated in Fig. 14. According to the large modulation amplitudes of the Cu-O lengths in the chain, the bond valences and the BVS of Cu(1) are remarkably modulated in the *t* space, which is distinct from those obtained for the Cu(2) atom in the Cu_2O_3 ladder (see Fig. 8). The BVS value of Cu(1) modulates between 1.9 and 3.1, which means that valence modulation including Cu^{2+} and Cu^{3+} ions occurs in the CuO_2 chain in $(Sr_2Cu_2O_3)_{0.70}CuO_2$. Because the valence modulation is brought about by the structural modulation, that is, by the large modulation of the Cu-O bonds in the CuO_2 chain, the holes prepared in the CuO_2 seem to be localized as the optical conductivity measurement has suggested.[28] The large modulation of BVS of Cu in the CuO_2 chain was also observed in Ca-rich

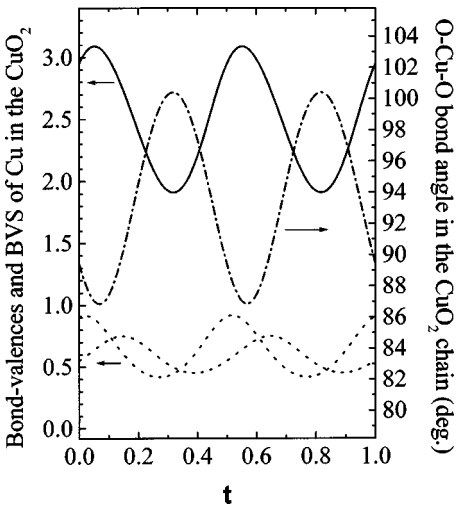

FIG. 14. Bond valences of Cu-O (dotted lines) and bond-valence sum (solid line) of Cu in the CuO_2 chain in $(Sr_2Cu_2O_3)_{0.70}CuO_2$. There is the correlation between the bond-valence sum of Cu and the O-Cu-O bond angle (dashed-and-dotted line) in the CuO_2 chain.

$(Sr_{0.057}Ca_{1.943}Cu_2O_3)_{0.70+\delta}CuO_2$,[42] but the behavior of the BVS wave is quite different from that obtained in $(Sr_2Cu_2O_3)_{0.70}CuO_2$. In addition, its BVS value is in the range of about 1.7–2.8. Presumably, the decrease of the BVS value in $(Sr_{0.057}Ca_{1.943}Cu_2O_3)_{0.70+\delta}CuO_2$ is mainly caused by the hole transfer from the CuO_2 chain to the Cu_2O_3 ladder about 0.2 holes per Cu atom in the Cu_2O_3. In any case, it has become apparent in the $(Sr_{2-x}Ca_xCu_2O_3)_{0.70+\delta}CuO_2$ series that large amounts of holes are formed in the CuO_2 chain by the large modulation of the Cu-O bonds. Especially in $(Sr_2Cu_2O_3)_{0.70}CuO_2$, the modulation of the Cu-O bonds are characteristically induced solely by the O atom in the CuO_2 chain. The large modulation of the O atom in the CuO_2 chain neatly brings about the valence modulation, namely, the hole localization in the modulated CuO_2 and the hole transfer to the Cu_2O_3 ladder. It is noteworthy that small amounts of holes on the Cu_2O_3 ladder, which is transferred through the O atom in the CuO_2 chain, are necessary to explain the semiconductive behavior of $(Sr_2Cu_2O_3)_{0.70}CuO_2$.[26,44] Thus the structural features of $(Sr_2Cu_2O_3)_{0.70}CuO_2$ obtained in the present study explicitly improve that picture proposed by Carter *et al.* which suggests that the holes prepared in the CuO_2 chain are mobile and responsible for the electrical properties of $(Sr_2Cu_2O_3)_{0.70}CuO_2$.[16]

D. Hole ordering in the modulated CuO_2 in $(Sr_2Cu_2O_3)_{0.70}CuO_2$

As clarified by the BVS calculations, most of the holes in $(Sr_2Cu_2O_3)_{0.70}CuO_2$ are located in the CuO_2 chain and the hole localization including Cu^{2+} and Cu^{3+} ions certainly occurs at room temperature. The hole localization seems to be related to charge-ordering behavior in the CuO_2 observed below 250 K,[16,45,46] whereas spin-gap behavior accompanied by the formation of the spin-dimerized state is realized at low temperature below 85 K.[9] Thus far some models of the hole-ordered structure which is considered to be closely responsible for the spin-dimerized state of the CuO_2 chain have been proposed. According to the initial studies with inelastic neutron-scattering measurement,[10] it was suggested that the Cu^{2+} ion couples with next-nearest-neighbor Cu^{2+} in the CuO_2 chain to form a periodic $\langle\uparrow(Cu^{2+})\rangle$-$\langle 0(Cu^{3+})\rangle$-$\langle\downarrow(Cu^{2+})\rangle$-$\langle 0(Cu^{3+})\rangle$-$\langle\uparrow(Cu^{2+})\rangle$ spin chain. The periodic structure of the spin arrangement might be attained if the periodicity of the hole-ordered structure were two units of the average substructure of the CuO_2 chain. In spite of the spin arrangement, Cox *et al.* suggested a superstructure with four times periodicity of the average CuO_2 along the *c* axis by x-ray-diffraction measurement.[17] Further, they proposed the domain structure with $\langle\uparrow\rangle$-$\langle 0\rangle$-$\langle\downarrow\rangle$-$\langle 0\rangle$-$\langle\uparrow\rangle$ and $\langle\uparrow\rangle$-$\langle\downarrow\rangle$-$\langle\uparrow\rangle$ in the spin-dimerized state of the CuO_2 chain. On the other hand, in conflict with their results, Fukuda *et al.* found the weak satellite reflections by the x-ray diffraction that are attributed to the superstructure with five times periodicity of the average CuO_2.[18] The apparent discrepancy between their results seems to come from the fact that they have observed only 00*l* reflections and that the number of x-ray data is insufficient to refine the structure parameters of the CuO_2 chain. Moreover, they have ignored the structural modulations in $(Sr_2Cu_2O_3)_{0.70}CuO_2$. Thus their superstructure models seem unsatisfactory to explain the occurrence of the hole-ordered state of the CuO_2 chain. We must note that the well refined hole-ordered structure in the plane of the CuO_2 chains in $(Sr_2Cu_2O_3)_{0.70}CuO_2$ has not been so far proposed at all. It should be emphasized that the most accurate model of the hole ordering in the CuO_2 is obtained by investigating the modulated structure of $(Sr_2Cu_2O_3)_{0.70}CuO_2$.

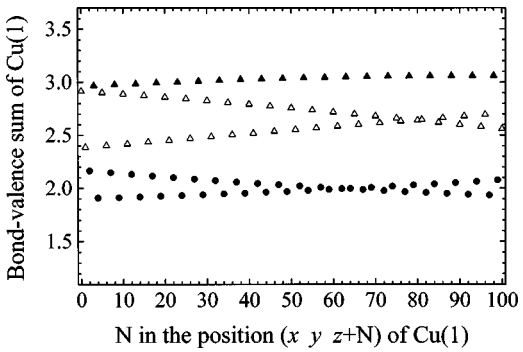

FIG. 15. Bond-valence sums of Cu(1) in the CuO_2 chain in the three-dimensional physical space. The solid circles show hole-unoccupied Cu^{2+} (dimer) sites; the solid triangles are fully hole-occupied (ZR-singlet) sites between the Cu^{2+} sites; the open triangles indicate partially hole-occupied (extended ZR-singlet) sites between dimers.

To investigate the hole-ordering behavior in the CuO_2 chain, it is necessary to transform the BVS values of the Cu(1) atom in the *t* space into those in the three-dimensional physical space. As we can see from Fig. 15, a hole-ordered structure including Cu^{2+} and Cu^{3+} ions is obtained in the CuO_2 chain in $(Sr_2Cu_2O_3)_{0.70}CuO_2$, though fluctuation of BVS values are observed to some extent. The fluctuation of BVS may be depressed with decreasing temperature. In the

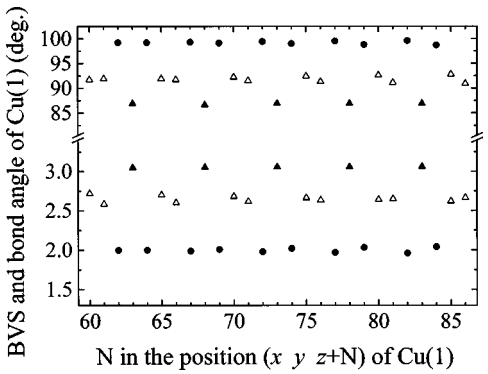

FIG. 16. Bond-valence sums and bond angles of Cu(1) in the CuO_2 chain in the three-dimensional physical space. The solid circles show hole-unoccupied Cu^{2+} (dimer) sites; the solid triangles are fully hole-occupied (ZR-singlet) sites between the Cu^{2+} sites; the open triangles indicate partially hole-occupied (extended ZR-singlet) sites between dimers.

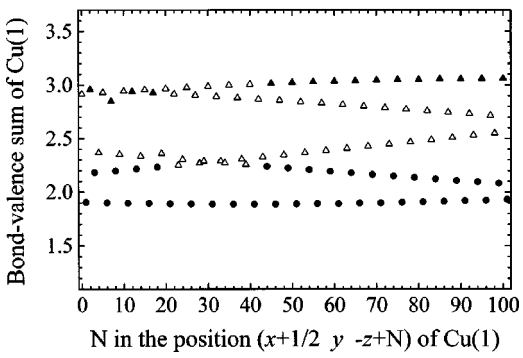

FIG. 17. Bond-valence sums of Cu(1) in the neighboring CuO_2 chain in the three-dimensional physical space. The solid circles show hole-unoccupied Cu^{2+} (dimer) sites; the solid triangles are fully hole-occupied (ZR-singlet) sites between the Cu^{2+} sites; the open triangles indicate partially hole-occupied (extended ZR-singlet) sites between dimers.

hole-ordered state at room temperature, it is indicated that the $\langle Cu^{2+}\rangle$-$\langle Cu^{3+}\rangle$-$\langle Cu^{2+}\rangle$ arrangement is present with the periodicity of five units of the average CuO_2 along the *c* axis. We can expect that the hole-ordered structure satisfactorily leads to the spin-dimerized state at low temperature, because $(Sr_2Cu_2O_3)_{0.70}CuO_2$ does not show structural transformation below room temperature. Details of the spin-dimerized state have been revealed mainly by Takigawa *et al.* and Eccleston *et al.* By ^{63,65}Cu NMR/NQR measurements, Takigawa *et al.* have successfully distinguished magnetic Cu^{2+} ions from nonmagnetic Cu^{3+}, which form Zhang-Rice (ZR) singlet.[12] They have suggested that the dimer with $\langle\uparrow(Cu^{2+})\rangle$-$\langle 0(Cu^{3+})\rangle$-$\langle\downarrow(Cu^{2+})\rangle$ spin fragment is formed in the CuO_2 chain in $(Sr_2Cu_2O_3)_{0.70}CuO_2$. Eccleston *et al.*, by inelastic neutron-scattering method, have revealed that the spin dimer with $\langle\uparrow\rangle$-$\langle 0\rangle$-$\langle\downarrow\rangle$ fragment has a periodicity of five units of the average CuO_2 chain along the *c* axis.[13] Taking into account the hole-ordered structure determined in the present work, we can conclude that the Cu^{2+} ion couples across Cu^{3+} with next-nearest-neighbor Cu^{2+} antiferromagnetically to form the periodic structure $\langle\uparrow(Cu^{2+})\rangle$-$\langle 0(Cu^{3+})\rangle$-$\langle\downarrow(Cu^{2+})\rangle$-$\langle 0\rangle$-$\langle 0\rangle$-$\langle\downarrow(Cu^{2+})\rangle$-$\langle 0(Cu^{3+})\rangle$-$\langle\uparrow(Cu^{2+})\rangle$-$\langle 0\rangle$-$\langle 0\rangle$ in the CuO_2 chain.

As we can see from Fig. 15, the Cu^{3+} between the Cu^{2+} ions seems quite stable in the CuO_2 chain. In other words, the nonmagnetic ZR singlet in the $\langle\uparrow\rangle$-$\langle 0\rangle$-$\langle\downarrow\rangle$ may be more stable than the extended ZR singlet[12] between $\langle\uparrow\rangle$-$\langle 0\rangle$-$\langle\downarrow\rangle$ dimers. Since the average valence of Cu in the modulated CuO_2 chain is 2.55, the amount of holes in the CuO_2 are insufficient to distribute themselves to make the complete sequence of -$\langle Cu^{2+}\rangle$-$\langle Cu^{3+}\rangle$-$\langle Cu^{2+}\rangle$-$\langle Cu^{3+}\rangle$-$\langle Cu^{3+}\rangle$-, where the extended ZR-singlet site, together with the ZR-singlet site, is fully included. In spite of the fluctuation of the BVS values at the extended ZR-singlet sites, the BVS of $\langle Cu^{2+}\rangle$-$\langle Cu^{3+}\rangle$-$\langle Cu^{2+}\rangle$ fragment is rather stable, especially near the position of $(x\ y\ z+60)$. To see the hole-ordered structure of the CuO_2 chain in more detail, it is significant to note that there is a correlation between the BVS value of Cu(1) and the O(1)-Cu(1)-O(1) bond angle in the CuO_2 chain (see Figs. 7 and 14). The BVS value of Cu(1) increases with decreasing the O(1)-Cu(1)-O(1) angle. As we can see from Fig. 16, the bond angles of O-Cu-O at the ZR-singlet site and the extended ZR-singlet site are about 87° and 92°, respectively, near the position of $(x\ y\ z+60)$. These are much close to 90° than the bond angles of O-Cu-O at the Cu^{2+} dimer sites in the CuO_2 chain. The O-Cu-O angle in the $Cu^{2+}O_4$ unit extends to about 99°. Accordingly, we can say that the CuO_4 unit at the ZR-singlet site has a tendency to make rectangle in the CuO_2 chain in $(Sr_2Cu_2O_3)_{0.70}CuO_2$. The rectangular CuO_4 unit at the ZR-singlet site in the CuO_2 chain is analogous to the local CuO_4 coordination in the CuO_2 plane of high-T_c cuprates.

It is much important, subsequently, to determine the two-dimensional configuration of the spin dimers in the plane of the CuO_2 chains in $(Sr_2Cu_2O_3)_{0.70}CuO_2$. We can estimate the two-dimensional configuration of the spin dimers from the two-dimensional hole-ordered structure in the CuO_2 plane in the modulated $(Sr_2Cu_2O_3)_{0.70}CuO_2$. Therefore the BVS calculations of Cu(1) at the site of $(x+\frac{1}{2}\ y\ -z+N)$ in the neighboring CuO_2 chain were performed in the same manner as the Cu(1) at $(x\ y\ z+N)$. In the neighboring CuO_2 chain also, as we can see from Fig. 17, the hole ordering with $\langle Cu^{2+}\rangle$-$\langle Cu^{3+}\rangle$-$\langle Cu^{2+}\rangle$ arrangement is present with the periodicity of five units of the average CuO_2. By considering some fluctuation, however, the $\langle Cu^{2+}\rangle$-$\langle Cu^{3+}\rangle$-$\langle Cu^{2+}\rangle$ arrangement seems to be interrupted near the position of $(x+\frac{1}{2}\ y\ -z+30)$. In this area, we can find the discommensuration with hole ordering, that is, the change of the $\langle Cu^{2+}\rangle$-$\langle Cu^{3+}\rangle$-$\langle Cu^{2+}\rangle$ arrangement. In addition, from the absence of the nearest-neighbor Cu^{2+} ions in the CuO_2 chain, we can understand that it is impossible to make ferromagnetic interaction between the nearest-neighbor Cu spins. Thus it has become apparent that antiferromagnetic interaction between the next-nearest-neighbor Cu spins in the $\langle\uparrow(Cu^{2+})\rangle$-$\langle 0(Cu^{3+})\rangle$-$\langle\downarrow(Cu^{2+})\rangle$ dimer is predominant in the CuO_2 chain. By theoretical calculations, Mizuno *et al.* indicated that the antiferromagnetic interaction between the next-nearest-neighbor Cu spins does not depend on the angle of the Cu-O-O-Cu path in the modulated CuO_2 chain.[35] Be-

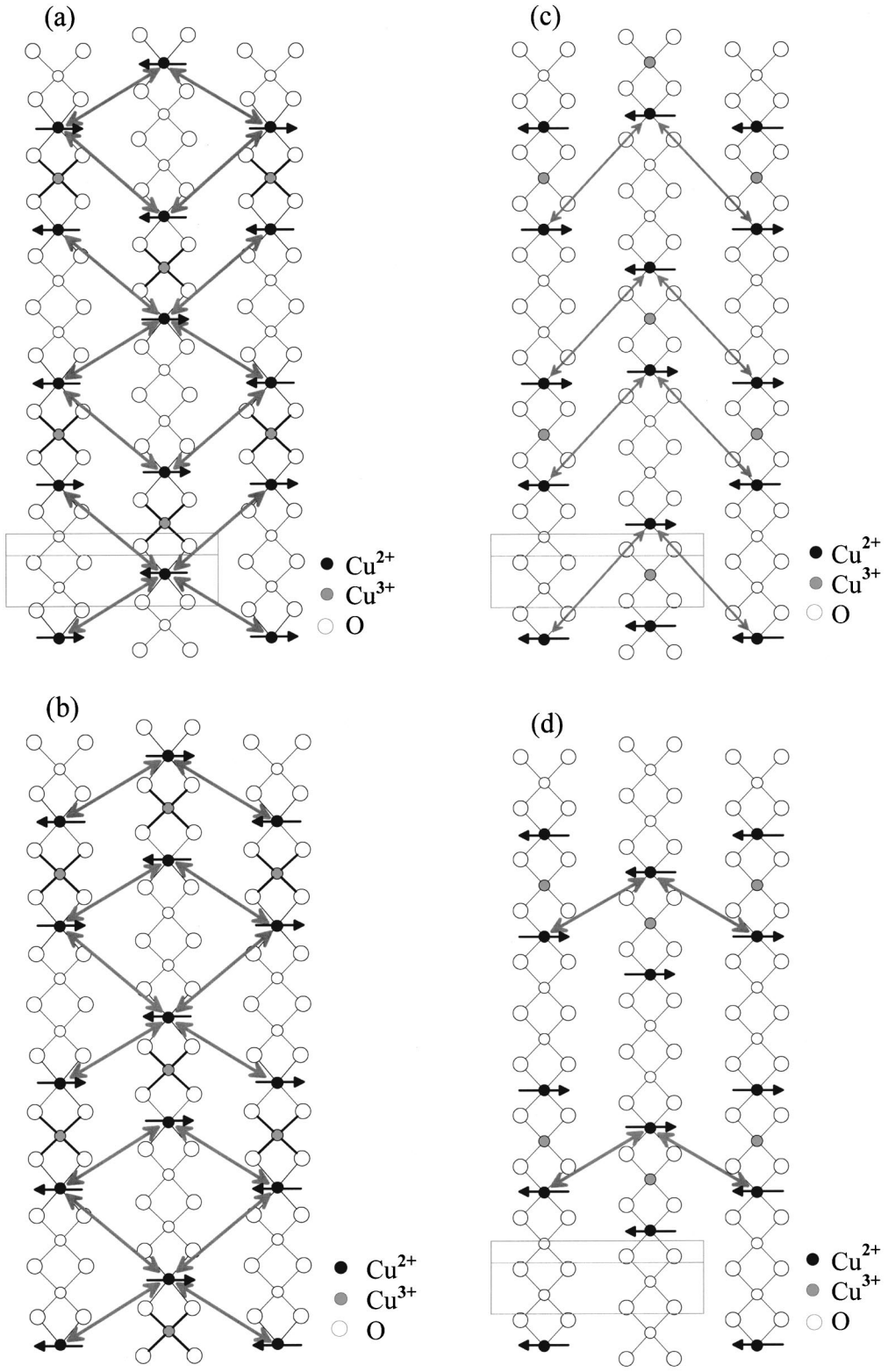

FIG. 18. The possible models of the two-dimensional hole-ordered CuO_2 plane in $(Sr_2Cu_2O_3)_{0.70}CuO_2$. Our models [(a) and (b)] are obtained by the bond-valence sum method with the modulated structure analysis. Models (c) and (d) are proposed by Regnault *et al.* and Matsuda *et al.*, respectively, by the inelastic neutron-scattering method. In all models, effective antiferromagnetic interactions through the quasistraight Cu-O-O-Cu paths between spin dimers in the neighboring CuO_2 chains are drawn by gray-colored arrows. In our models of the hole-ordered structure, the antiferromagnetic interaction through quasistraight Cu-O-O-Cu paths between the dimers in the neighboring CuO_2 chains can be obtained most effectively.

cause of the discommensuration, two kinds of hole-ordered structures are possible in the modulated CuO_2 plane in $(Sr_2Cu_2O_3)_{0.70}CuO_2$. Figures 18(a) and (b) show the two-dimensional hole-ordered structures in the CuO_2 plane back and forth the discommensuration around the $(x+\frac{1}{2}\ y\ -z+30)$, respectively. For comparison, other possible models of hole-ordered structure for the spin-dimerized state proposed by Regnault *et al.* and Matsuda *et al.* by inelastic neutron-scattering method[14,15] are presented together in Figs. 18(c) and (d). The essential difference among these models is the mode of relative arrangements of the $\langle\uparrow\rangle$-$\langle 0\rangle$-$\langle\downarrow\rangle$ dimers between neighboring CuO_2 chains. The most appropriate model of the two-dimensional configuration of the magnetic dimers should contain the most effective interchain interaction between the neighboring CuO_2 chains. As in the case of $(Sr_{0.057}Ca_{1.943}Cu_2O_3)_{0.70+\delta}CuO_2$,[47] the interdimer interaction between the neighboring CuO_2 chains seems to give the most important interchain interaction because the dimers contain almost all of the magnetic Cu^{2+} ions in the CuO_2. In our models of the hole-ordered structure, the antiferromagnetic interaction through quasistraight Cu-O-O-Cu paths between the dimers in the neighboring CuO_2 chains can be obtained most effectively [see Figs. 18(a) and (b)]. In other models, the antiferromagnetic interaction seems to be weak or sparsely contained [see Figs. 18(c) and (d)]. From the theoretical consideration,[35] the antiferromagnetic interaction through the quasistraight Cu-O-O-Cu paths between the CuO_2 chains is caused by the overlap between the $3dx^2-y^2$ orbital of Cu and the $2p_\sigma$ orbital of O in the CuO_2. With the antiferromagnetic interaction between the neighboring CuO_2 chains, further, we can assign the ferromagnetic interdimer interaction in the CuO_2 chain as $\langle\uparrow\rangle$-$\langle 0\rangle$-$\langle\downarrow\rangle$-$\langle 0\rangle$-$\langle 0\rangle$-$\langle\downarrow\rangle$-$\langle 0\rangle$-$\langle\uparrow\rangle$. The resulting ferromagnetic interdimer interaction in the chain is compatible with the experimental results by the inelastic neutron-scattering method.[13–15] In this way, the two-dimensional configuration of the spin dimers has been successfully obtained from the hole-ordered structure in the CuO_2 plane, where the valence of the Cu atom is well controlled by the modulation of the O atom in the CuO_2 chain in $(Sr_2Cu_2O_3)_{0.70}CuO_2$. The hole-ordered structure in the CuO_2 plane in $(Sr_2Cu_2O_3)_{0.70}CuO_2$ is much simpler than that proposed in Ca-rich $(Sr_{0.057}Ca_{1.943}Cu_2O_3)_{0.70+\delta}CuO_2$.[47] The valence modulation and the hole-ordering behavior in the CuO_2 chain in the Ca-rich $Sr_{14-x}Ca_xCu_{24}O_{41}$ compounds seem to show more complicated features because of the Cu atom modulated together with the O atom in the CuO_2 chain.

IV. SUMMARY

In the present study, the modulated composite structure of $(Sr_2Cu_2O_3)_{0.70}CuO_2$, "$Sr_{14}Cu_{24}O_{41}$," with the two-legged Cu_2O_3 ladder and the one-dimensional CuO_2 chains has been investigated at room temperature by the use of correct centrosymmetric $(3+1)$-dimensional superspace group. In the modulated composite structure of $(Sr_2Cu_2O_3)_{0.70}CuO_2$, displacive modulation of the O atom in the CuO_2 chain is fairly large. By the large modulation of the O atom, almost all of the holes are prepared in the CuO_2 chain. Considering the modulation of bond angles, it has been found that the Cu-O bond in the CuO_2 is tilting toward the Cu_2O_3 ladder in order that the O in the CuO_2 chain acts as apical oxygen for the CuO_4 square in the Cu_2O_3 ladder. The BVS calculation has indicated that the valence of Cu atom in the Cu_2O_3 ladder is $+2.04$, where about 0.03 holes are certainly transferred from the CuO_2 chain through the modulated O atom in the CuO_2. The Cu atoms in the hole-doped CuO_2 chain have been proved to form the hole-ordered structure with the next-nearest-neighbor Cu^{2+} ions separated by the Cu^{3+} ion on the ZR-singlet site. The periodicity of the hole-ordered CuO_2 chain along the *c* axis is five times that of the average CuO_2 lattice, which is compatible with the spin-dimerized state at low temperature. The new model of the two-dimensional hole-ordered structure in the CuO_2 plane has been obtained by the BVS method. Furthermore, the two-dimensional configuration of the spin dimers has been successfully derived from the hole-ordered structure in the CuO_2 plane. We can conclude that the role of the modulation of the O atom in the CuO_2 chain is to prepare and distribute holes in the CuO_2, that is, to control the valence of Cu atoms both in the Cu_2O_3 ladder and in the CuO_2 chain in $(Sr_2Cu_2O_3)_{0.70}CuO_2$.

[1] E. Dagotto, J. Riera, and D. Scalapino, Phys. Rev. B **45**, 5744 (1992).

[2] T. M. Rice, S. Gopalan, and M. Sigrist, Europhys. Lett. **23**, 445 (1993).

[3] For reviews, see E. Dagotto, Rep. Prog. Phys. **62**, 1525 (1999); E. Dagotto, J. Electron Spectrosc. Relat. Phenom. **117-118**, 223 (2001); K. M. Kojima, N. Motoyama, H. Eisaki, and S. Uchida, *ibid.* **117-118**, 237 (2001).

[4] M. Sigrist, T. M. Rice, and F. C. Zhang, Phys. Rev. B **49**, 12 058 (1994).

[5] T. Nagata, M. Uehara, J. Goto, J. Akimitsu, N. Motoyama, H. Eisaki, S. Uchida, H. Takahashi, T. Nakanishi, and N. Mori, Phys. Rev. Lett. **81**, 1090 (1998).

[6] M. Uehara, T. Nagata, J. Akimitsu, H. Takahashi, N. Mori, and K. Kinoshita, J. Phys. Soc. Jpn. **65**, 2764 (1996).

[7] A. Janner and T. Janssen, Acta Crystallogr., Sect. A: Cryst. Phys., Diffr., Theor. Gen. Crystallogr. **A36**, 408 (1980).

[8] E. M. McCarron, M. A. Subramanian, J. C. Calabrese, and R. L. Harlow, Mater. Res. Bull. **23**, 1355 (1988).

[9] M. Matsuda and K. Katsumata, Phys. Rev. B **53**, 12 201 (1996).

[10] M. Matsuda, K. Katsumata, H. Eisaki, N. Motoyama, S. Uchida, S. M. Shapiro, and G. Shirane, Phys. Rev. B **54**, 12 199 (1996).

[11] Z. Hiroi, S. Amelinckx, G. Van Tendeloo, and N. Kobayashi, Phys. Rev. B **54**, 15 849 (1996).

[12] M. Takigawa, N. Motoyama, H. Eisaki, and S. Uchida, Phys. Rev. B **57**, 1124 (1998).

[13] R. S. Eccleston, M. Uehara, J. Akimitsu, H. Eisaki, N. Motoyama, and S. Uchida, Phys. Rev. Lett. **81**, 1702 (1998).

[14] L. P. Regnault, J. P. Boucher, H. Moudden, J. E. Lorenzo, A. Hiess, U. Ammerahl, G. Dhalenne, and A. Revcolevschi, Phys.

Rev. B **59**, 1055 (1999).
[15] M. Matsuda, T. Yosihama, K. Kakurai, and G. Shirane, Phys. Rev. B **59**, 1060 (1999).
[16] S. A. Carter, B. Batlogg, R. J. Cava, J. J. Krajewski, W. F. Peck, Jr., and T. M. Rice, Phys. Rev. Lett. **77**, 1378 (1996).
[17] D. E. Cox, T. Iglesias, K. Hirota, G. Shirane, M. Matsuda, N. Motoyama, H. Eisaki, and S. Uchida, Phys. Rev. B **57**, 10 750 (1998).
[18] T. Fukuda, J. Mizuki, and M. Matsuda, Phys. Rev. B **66**, 012104 (2002).
[19] P. M. de Wolff, T. Janssen, and A. Janner, Acta Crystallogr., Sect. A: Cryst. Phys., Diffr., Theor. Gen. Crystallogr. **A37**, 625 (1980).
[20] A. Yamamoto, Acta Crystallogr., Sect. A: Found. Crystallogr. **A48**, 476 (1992).
[21] K. Ukei, T. Shishido, and T. Fukuda, Acta Crystallogr., Sect. B: Struct. Sci. **B50**, 42 (1994).
[22] A. F. Jensen, V. Petricek, F. K. Larsen, and E. M. McCarron, Acta Crystallogr., Sect. B: Struct. Sci. **B53**, 125 (1997).
[23] T. Ohta, F. Izumi, M. Onoda, M. Isobe, E. Takayama-Muromachi, and A. Hewat, J. Phys. Soc. Jpn. **66**, 3107 (1997).
[24] M. Kato, T. Adachi, and Y. Koike, Physica C **265**, 107 (1996).
[25] M. Matsuda, K. Katsumata, T. Osafune, N. Motoyama, H. Eisaki, S. Uchida, T. Yokoo, S. M. Shapiro, G. Shirane, and J. L. Zarestky, Phys. Rev. B **56**, 14 499 (1997).
[26] N. Motoyama, T. Osafune, T. Kakeshita, H. Eisaki, and S. Uchida, Phys. Rev. B **55**, R3386 (1997).
[27] N. Motoyama, H. Eisaki, S. Uchida, N. Takeshita, N. Mori, T. Nakanishi, and H. Takahashi, Europhys. Lett. **58**, 758 (2002).
[28] T. Osafune, N. Motoyama, H. Eisaki, and S. Uchida, Phys. Rev. Lett. **78**, 1980 (1997).
[29] K. Kato, Acta Crystallogr., Sect. A: Found. Crystallogr. **A50**, 351 (1994).
[30] D. T. Cromer and J. B. Mann, Acta Crystallogr., Sect. A: Cryst. Phys., Diffr., Theor. Gen. Crystallogr. **A24**, 321 (1968).
[31] D. T. Cromer and D. Liberman, J. Chem. Phys. **53**, 1891 (1970).
[32] M. Terauchi (unpublished).
[33] K. Kato, Acta Crystallogr., Sect. B: Struct. Sci. **B46**, 39 (1990).
[34] B. Gorshunov, P. Haas, T. Room, M. Dressel, T. Vuletic, B. Korin-Hamzic, and S. Tomic, Phys. Rev. B **66**, 060508(R) (2002).
[35] Y. Mizuno, T. Tohyama, S. Maekawa, T. Osafune, N. Motoyama, H. Eisaki, and S. Uchida, Phys. Rev. B **57**, 5326 (1998).
[36] R. J. Cava, A. W. Hewat, E. A. Hewat, B. Batlogg, M. Marezio, K. M. Rabe, J. J. Krajewski, W. F. Peck, and L. W. Rupp, Physica C **165**, 419 (1990).
[37] I. D. Brown, J. Solid State Chem. **82**, 122 (1989).
[38] M. Kato, K. Shiota, and Y. Koike, Physica C **258**, 284 (1996).
[39] I. D. Brown and D. Altermatt, Acta Crystallogr., Sect. B: Struct. Sci. **B41**, 244 (1985).
[40] T. Takahashi, T. Yokoya, A. Ashihara, O. Akaki, H. Fujisawa, A. Chainani, M. Uehara, T. Nagata, and J. Akimitsu, Phys. Rev. B **56**, 7870 (1997).
[41] M. Arai and H. Tsunetsugu, Phys. Rev. B **56**, R4305 (1997).
[42] M. Isobe and E. Takayama-Muromachi, J. Phys. Soc. Jpn. **67**, 3119 (1998).
[43] N. Nucker, M. Merz, C. A. Kuntscher, S. Gerhold, S. Schuppler, R. Neudert, M. S. Golden, J. Fink, D. Schild, S. Stadler, V. Chakarian, J. Freeland, Y. U. Idzerda, K. Conder, M. Uehara, T. Nagata, J. Goto, J. Akimitsu, N. Motoyama, H. Eisaki, S. Uchida, U. Ammerahl, and A. Revcolevschi, Phys. Rev. B **62**, 14 384 (2000).
[44] M. W. McElfresh, J. M. D. Coey, P. Strobel, and S. von Molnar, Phys. Rev. B **40**, 825 (1989).
[45] Z. V. Popovic, M. J. Konstantinovic, V. A. Ivanov, O. P. Khuong, R. Gajic, A. Vietkin, and V. V. Moshchalkov, Phys. Rev. B **62**, 4963 (2000).
[46] V. Kataev, K. Y. Choi, M. Gruninger, U. Ammerahl, B. Buchner, A. Freimuth, and A. Revcolevschi, Phys. Rev. B **64**, 104422 (2001).
[47] M. Isobe, M. Onoda, T. Ohta, F. Izumi, K. Kimoto, E. Takayama-Muromachi, A. W. Hewat, and K. Ohoyama, Phys. Rev. B **62**, 11 667 (2000).